Journal of Applied Fluid Mechanics, Vol. 9, No. 5, pp. 2359-2367, 2016.
Available online at www.jafmonline.net, ISSN 1735-3572, EISSN 1735-3645.
DOI:10.18869/acadpub.jafm.68.236.25382

Analysis of the Effect of the Swirl Flow Intensity on Combustion Characteristics in Liquid Fuel Powered Confined Swirling Flames

M. Klančišar[1†], T. Schloen[1], M. Hriberšek[2] and N. Samec[2]

[1]*Department of research and development, Max Weishaupt GmbH, Schwendi, Germany*
[2]*University of Maribor, Faculty of mechanical engineering, Maribor, Slovenia*

†*Corresponding Author Email: fg.klancisar@weishaupt.de*

(Received July 29, 2015; accepted December 11, 2015)

ABSTRACT

This article examines the implementation of CFD technology in the design of the industrial liquid fuel powered swirl flame burner. The coupling between the flow field and the combustion model is based on the eddy dissipation model. The choice of the LES (Large Eddy Simulation) turbulence model over standard RANS (Reynolds Averaged Navier-Stokes) offers a possibility to improve the quality of the combustion-flow field interaction. The Wall Adapting Local Eddy-Viscosity (WALE) sub-grid model was used. The reaction chemistry is a simple infinitely fast one step global irreversible reaction. The computational model was setup with the Ansys-CFX software. Through the detailed measurements of industrial size burner, it was possible to determine the natural operational state of the burner according to the type of fuel used. For the inlet conditions, axial and radial velocity components were calculated from known physical characteristics of both the fuel and air input, with the initial tangential velocity of the fuel assumed as18% of the initial axial fuel velocity. Different swirl number (S) values were studied. Addition of a surplus (in comparison to conventional flame stabilization) of tangential air velocity component (W), the rotational component increases itself with a considerably high magnitude, contributing to the overall flame stabilization. The level of S especially influences the turbulent energy, its dissipation rate and turbulent (Reynolds) stresses. In the case of high swirl number values (S > 0,65) it is possible to divide the flow field in three principle areas: mixing area (fuel-air), where exothermal reactions are taking place, central recirculation area and outer recirculation area, which primarily contains the flow of burnt flue gases. The described model was used to determine the flow and chemical behavior, whereas the liquid atomization was accounted for by LISA (Linear Instability Sheet Atomization) model incorporating also the cavitation within injection boundary condition. The boundary conditions were determined based on the data from the experimental hot water system. Depending on system requirements, especially with continuous physical processes as well as the results of experimental measurements, the paper reports on determination of the mixing field and its intensity in the turbulent flow, the description of heat release and interaction of turbulent flow field and chemical kinetics in the case of confined swirling flames.

Keywords: CFD; Fluid dispersion; Combustion; Industrial burner; Confined swirling flame; Two-phase flow.

1. INTRODUCTION

Development of industrial size burners is commonly associated with careful design and extensive testing procedures. Although testing is indispensable in development of an industrial burner, numerical simulation of reactive transport phenomena inside a burner can help significantly in cutting the development phase. In recent years, development of Computational Fluid Dynamics (CFD) based simulation tools has reached a level that enables its use also in the framework of development of industrial size burners, without a limitation to only steady state solutions, which is mainly attributed to the strong development of Large Eddy Simulation models of turbulent flow in the CFD. Combined with chemistry models of combustion reactions and models, linking the chemistry dynamics scale and flow scale, this represents a powerful tool for analysis of the combustion processes in an industrial burner.

2. COMBUSTION PROCESS MODELING IN INDUSTRIAL BURNER

Combustion as a physical phenomenon combines several complex phenomena: compressible turbulent

flow, heat and mass transfer as well as chemical reactions. Whereas chemical reactions occur at a molecular level, the conditions, under which they take place, are dominated by phenomena on a macroscopic level, the most important of all being turbulent flow. Turbulence is in itself probably one of the most complex phenomena of non-reactive flow. There are different temporal and dimensional scales combined, which are a cause for many open questions on the interaction with turbulence. Turbulent combustion is the result of two-way interaction of turbulence and chemical processes. When the flame is interacting with a turbulent flow, it is altered due to the strong flow accelerations initiated due to the heat transfer and strong changes in kinematic viscosity. This mechanism can produce the so-called turbulence in the reactive flow, or the mentioned turbulence could be damped ("relaminarization" due to the combustion process). On the other hand, the turbulence is constantly changing the structure of the flame which otherwise can improve the combustion process. When developing a swirl flame burner, the flow phenomena has an even greater impact on combustion performance as in classical burners. It is therefore of great importance to set up a computational model, capable of capturing the main physical effects, that govern the combustion process. In the following, detailed information on the computational model, developed within the Ansys-CFX 14 solver, is given.

2.1 Turbulent Flow

The turbulence can be characterized by fluctuations of local properties. It occurs at a relatively high Reynolds numbers, depending on the geometry of the system. When quantitatively describing turbulence, flow and turbulence quantities are usually split into a resolved and modeled part as described by Gerlinger, P. (2005). In most cases of simulation of industrial problems, the Reynolds averaged Navier-Stokes equations are used, i.e. splitting the solution into time averaged field and oscillating contribution. As high swirling flows in confined geometry are characterized by oscillations of flow in time, it is more advisable to use the Large Eddy Simulation type model of turbulence. In our case, in the context of LES, the Wall Adapting Local Eddy-Viscosity (WALE) sub-grid model was applied, as it is recommended for the use in complex geometries (Klančišar, *et al.* 2013).Mathematically, the velocity field is separated into a resolved part and sub-grid part. The resolved part represents the large eddies, hence the sub-grid the small scales whose effect is included through sub-grid scale model (in principle the filtering kernel). The filtered equations are derived from Navier-Stokes equation of motion for incompressible flow as summarized from Liu Z., (2010):

$$\frac{\partial u_i}{\partial t} + u_j \frac{\partial u_i}{\partial x_j} = -\frac{1}{\rho}\frac{\partial p}{\partial x_i} + \frac{\partial}{\partial x_j}\left(\nu \frac{\partial u_i}{\partial x_j}\right) \quad (1)$$

Sub-grid scale flow (turbulence) usually contains the Boussinesq hypothesis and seeks to calculate the sub-grid scale stress using the rate of stress tensor. When all of the above mentioned is derived into the filtered Navier-Stokes equation (Eq. 1) we get:

$$\frac{\partial \overline{u_i}}{\partial t} + \overline{u_j}\frac{\partial \overline{u_i}}{\partial x_j} = -\frac{1}{\rho}\frac{\partial \bar{p}}{\partial x_i} + \frac{\partial}{\partial x_j}\left(\nu \frac{\partial \overline{u_i}}{\partial x_j}\right) \quad (2)$$

In order to assess the extent of rotational component of the flow field, the global vorticity (swirl) number S is introduced:

$$S = \frac{\int_0^{R_{in}} wur^2 dr}{R_{in}\int_0^{R_{in}} u^2 r dr} \quad (3)$$

where w is the tangential velocity component and u the longitudinal (axial) velocity component. By adjusting the tangential flow velocity different vortical flow fields can be achieved, which consequently affects the combustion conditions in the burner (Fig. 1).

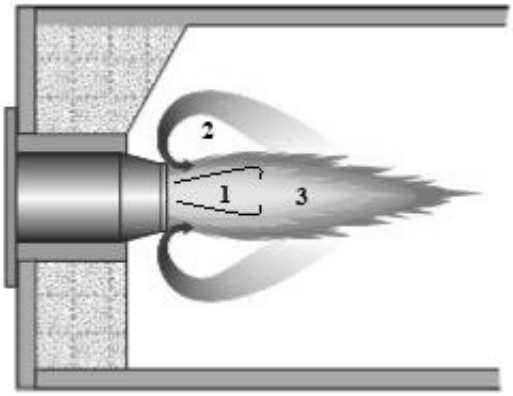

Fig. 1. General swirl geometry (1 – internal recirculation region, 2 – external recirculation region, 3 – reactive region).

The LES based simulation of turbulent flow requires dense computational grids. To compare the quality of the results, we used three non-uniform computational meshes. On mesh 2, we used detailed discretization in the vicinity of the inlet points (air and fuel inlet, swirl blades) to achieve high resolution and at the same time to reduce the computational time (we observed the flame process mainly in its mixing zone). The characteristics of the three different meshes are shown in Table 1.

Table 1 Mesh characteristics

	Comput. grid 1	Comput. grid 2	Comput. grid 3
Node count	228315	2251218	7523986
Element count	979471	12410198	23324356

For approximation of the minimal node count we can use the following expression:

$$N_{LES} \geq \frac{5 \cdot 1{,}5}{60\pi} \cdot Re^{3/4} \quad (4)$$

And for our case (Re between 10^4 and 10^5) the minimal node count:

Table 2 Minimal node count

Re	N_{LES}
10^4	40^3
10^5	224^3
10^6	1258^3
10^7	7079^3

Apart of the above described, we verified the meshes also with the physical quantity. At first we simulated "cold" flow (without combustion) to compare the velocity profiles for all three meshes. At stage two, we observed the flame temperature. We abandoned mesh 1 right after the second stage; the velocity profiles (cold flow) were way off (over 30% error around the inlet domain part) even with the comparison to conventional swirl number of 0.5and the simulation also diverged with the coupling of the combustion model. The second mesh (transient case) was used with success and after investigation and comparison to mesh 3 we concluded that the mesh 2 gives sufficient resolution of the vorticity, temperature generation and the species transport. As the mesh 2 is without detailed discretization in the second half (in the direction of the outlet) of the combustion chamber, we used the 7.5 million node mesh as in the future we want to observe also the chemical transport at the extinction point (better resolution for calculating the CO oxidation).

2.2 Chemical Reaction Rates

Chemical reactions are occurring at the molecular level, and their characteristic time is much shorter than the flow characteristic time. In order to accurately compute mass balances, the most important chemical reaction and rates of chemical reactions has to be specified. In our case a two stage chemical reactions were taken into account. The first stage was described by

$$C_{12}H_{23} + 11{,}75O_2 \rightarrow 12CO + 11{,}5H_2O \quad (5)$$

and the second stage by

$$CO + \frac{1}{2}O_2 \rightarrow CO_2 \quad (6)$$

In our case we used $C_{12}H_{23}$ (basically Diesel fuel) as pure substance, with the same properties as the heating oil (it evaporates in its equivalent gas phase). In the first stage of reaction the gas phase and oxygen are expressed as reactants with carbon monoxide and water as reaction products. In the second stage the oxygen stays as reactant with addition of carbon monoxide and carbon dioxide as the reaction product. Additionally, the chemical reaction rate (*RR*) has to be specified. In general it can be expressed by the temporal variation of the concentration of any compound reactants, or products as the rate of its formation. Based on the Law of mass action the rate of consumption of chemical compounds of a given reaction is proportional to their product concentration to the characteristic power, which is numerically equal to the stoichiometric coefficient. For a general description of chemical reactions, the Law of mass action can be written with the following mathematical form:

$$RR = k\prod_{i=1}^{N}[X_i]^{v_i'} \quad (7)$$

where k is the coefficient of proportionality or the specific rate constant of the chemical reaction, $[X_i]$ the concentration of the i-th component reacting mixture usually expressed in [mol/cm^3] and v_i' corresponding stoichiometric coefficient. The rate constant of the chemical reaction for a given reaction is independent of the concentrations of the individual components of the reacting mixture and it is only dependent on the temperature. Among different models, the Arrhenius equation is one of the most robust choices,

$$k = Aexp\left(-\frac{E_a}{R_m T}\right) \quad (8)$$

where factor A is typical for a given reaction (the values of the Arrhenius equation are set empirically), and the E_a is activation energy in our case 125604 J/mol. All the above described variables and parameters are also part of the EDM combustion model (with the fine tuning of the product limiter) which we used to solve the complexity of combustion.

2.3 Combustion-Flow Interaction

Given the fact that we are dealing with non-premixed turbulent flames, the analysis requires an appropriate strategy to link the turbulent mixing with the reactions of the main species (Kunio Terao, (2007) and Thomas Aumeier, (2011) and Faragó Z., (1985) and Ribera T, Faragó Z., (1996)).As mentioned before, the Eddy Dissipation Model or EDM (Ansys CFX 14.0, Solver theory guide) was sufficient for this purpose. EDM is based on assumption that the chemical reactions are clearly quicker that the transport phenomena. Products are generated parallel to the state when the reactants are mixed on molecular level. The model assumes that the reaction rate is time depended (the time needed to mix the reactants on molecular level). The mentioned time in the turbulent flow depends of the eddy properties. This concept is widely used for simulation of commercial combustion devices as the ratio between the chemical reactions and the mixing of the reactants is comparable. In EDM, rate of the progress of elementary reaction k is defined with:

- Reactant limiter

$$R_{i,r} = v'_{i,r}M_{w,i}A\rho\frac{\varepsilon}{k}min\left(\frac{Y_R}{v_{R,r}M_{w,R}}\right) \quad (9)$$

- Product limiter

$$R_{i,r} = v'_{i,r}M_{w,i}AB\rho\frac{\varepsilon}{k}\frac{\Sigma_P Y_P}{\sum_j^N v''_{j,r}M_{w,j}} \quad (10)$$

Where Y_P is the mass component of the product P, Y_R mass component of the reactive partner R, A and B empirical constants.

2.4 Liquid Fuel Dispersion

Fuel dispersion (Caraeni, D.*et al.* (2000) and Kunio

Terao, (2007) and Thomas Aumeier, (2011) and Faragó Z., (1985) and Z. Faragó, A. Baumann, (1990)), is essentially the conversion of the oil jet into the oil droplets (Fig. 4). Fuel jet starts to tear and disintegrate into tiny droplets of fuel after entering the combustion chamber (Fig. 2) as a result of the high-velocity jet and the heat released from the flame (Ribera T, Faragó Z., (1996) and Julie Parent, Z. Faragó, (1986) and Wolfgang Möllenbruck, (1990)).The mechanism of jet breakup has not yet been fully investigated. In the pressure nozzles jet exiting from the nozzle creates a cone, which is progressing through the volume to a certain end point. In it, the process of disintegration occurs, forming droplets of various sizes, which can also be smaller than the diameter of the nozzle, depending on the conditions of injection (W. Buschulte, W. Wedekamm, (1976) and Z. Faragó, B. Knapp (2000)).

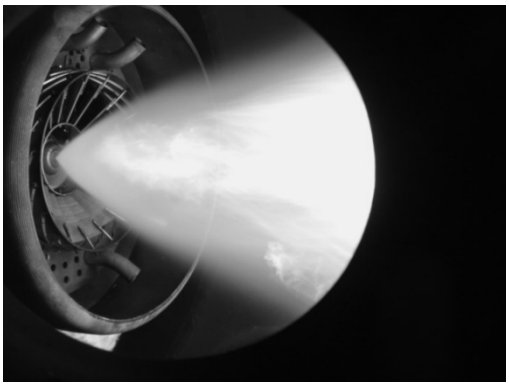

Fig. 2. Dispersion and an ignition of heating oil in the swirling flame.

The main task of the numerical model for the purpose of modeling the initial disintegration of a liquid fuel into droplets (Sridhara and Raghunandan 2010) is to determine the initial conditions at the exit of the injector. Satisfactory conditions are:

- Initial droplet diameter,
- Initial velocity components,
- Initial spray angle.

One of the most robust methods through which we can define inject conditions of a liquid fuel is the BLOB method (Zadravec, *et al.* (2014)); simple method, where the initial break-up of droplets and a detailed description of atomization of fuel are not taken into account. Droplets are assumed with constant round form. This method does not provide any additional configuration parameters and knowledge of the nozzle and is used to describe the basic approach to fuel injection through the nozzle.

For the description of the disintegration of a liquid fuel HHO we used BLOB method that has proven to be the most appropriate. For a description of the final disintegration of the oil droplets we used Schmehl breakup model (Ansys CFX 14.0, Solver theory guide). A lot of attention was paid to the size of the oil droplets. Mean diameter of the oil droplets is calculated using the empirical equation, which is used by the Schmehl numerical model. The largest oil droplets are at the beginning of the spray, where their size is in the range of 150 microns (Rosin-Rammler was used). Furthermore, oil droplets are disintegrating into even smaller in order to achieve the fineness of the spraying conditions. Oil droplets of such magnitude satisfactory reflect conditions in which the experiment was carried out.

3. SWIRL FLAME BURNER SETUP

The setup consists of a Weishaupt WKGL 80 1SFseries type swirl-burner mounted on the experimental hot water boiler. The mere entry of fuel (Fig. 3) is primarily associated with creating a vortex flow immediately at the exit of the injector. While the liquid fuel (heating oil) is distributed in the central burner part with the help of the mixing nozzle (conical form of oil spray), due to the inertness of the oil-cone, the formation of the turbulence can be partially ignored. On the other hand, a primary fuel (for example natural gas) enters through six injectors with the same geometry and with a constant pressure. In the same plane air phase is supplied through the vanes, defining the vortical flow field in the vicinity of the burner.

The whole experiment was carried out on the testing bench (Fig. 4) with the monitoring software. We used standard testing equipment for the flue gas analysis (electrochemical) and the cooled temperature probe for the temperature measurement inside the flame area. The swirl numbers were calculated using the known geometry of the swirl-generator and checked with the cold-flow simulations. To achieve the stable heat release, we used light oil without sulfur fraction.

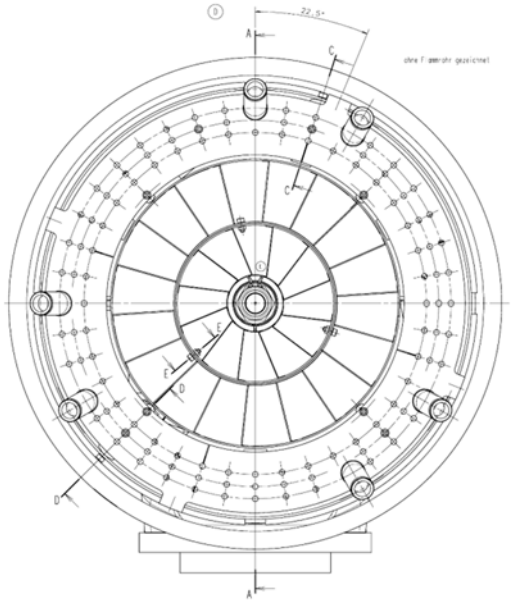

Fig. 3. Burner air/fuel distributor.

The burner that served in the experimental setup was producing 22 MW of heating power and had the operating parameters listed in Table 1.

Table 3 Operating parameters of swirling burner – heating oil experiment

Average fuel mass flow	0.51667 kg/s
Average air mass flow	8.25234 kg/s
Swirl number	0.5, 0.6, 0.75
Inlet air temperature	306.0 K
Absolute pressure	95500 Pa
Fuel-Air ratio (λ)	1.15
Static pressure - outlet	20 Pa
Average temperature – combustion chamber wall	343 K

In the case of oil dispersion, we assumed the following conditions in the combustion chamber equipped with conventional nozzles:

- Mean diameter of oil droplets: *150 μm*
- Amount of oil droplets in combustion chamber: $10^5 – 10^6$ *drop l./cm*^{3}

In order to assess the influence of the tangential flow velocity on the combustion in the burner several flow configurations were computed, including vorticity number values *S=0.5*, *S=0.6* and *S=0.75*. The value of *S = 0.5*is widely used with the conventional non-premixed burners; where the tangential flow component apart of being the flame stabilizing quantity, isn't used in terms of shorten the flame. Of course the conventional setup has served us as a basis for the realized semi- and

Fig. 4. Burner testing bench.

high swirl simulations. The *S = 0.6* is basically the value for the case where the flame in comparison with conventional burner, is shortened for approx. 25% of its original length. The flame becomes wider and we can observe the first axial flow fluctuations at the flame extinction point. High swirl state at *S = 0.75* brings us the 50% reduction in the flame length. The choice of the mentioned swirl numbers was plainly practical as the burner is by default adjusted to these values.

4. ANALYSIS OF RESULTS

4.1 Realized Simulations

Result of the movement of gas at the exit is the collapse of the global "laminar" flow. According to the experimental system and with the addition of the liquid fuel injection we can describe flow field solely without combustion. On the same plane as the fuel, the air is supplied at the same time with a strong rotational movement, which improves mixing and leads to virtually homogeneous two-phase flow. The mixture flows in a swirling movement to the external recirculation region and towards the end of the combustion chamber, shown in Fig.5. The effect of tangential air flow is clearly visible in Fig. 6. Problems arise when the mixture becomes reactive (Poinsot, T., Veynante, D. (2005) and Vervisch, L. (2005)), and chemical reactions begin to take place in the combustion chamber. In some unfavorable turbulator settings, pulsations or interactions of the flow waves with vortices occur (Zhang *et al.* 2009 and Klančišar e*t al.* 2015).

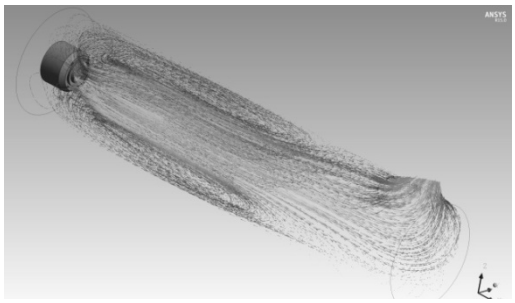

Fig. 5. Non-reactive flow field in 3-D.

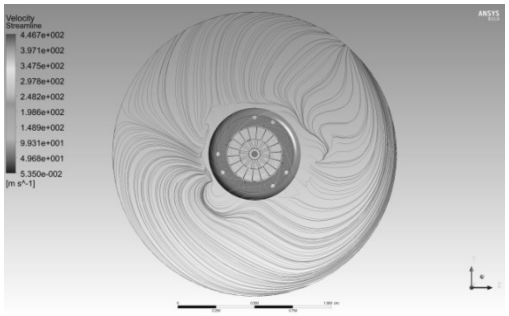

Fig. 6. Non-reactive recirculating flow field in the front view of the distributor.

For an overview of the global flow characteristics in the fully developed flow, the system can be displayed through a normalized flow function for counter-rotating configuration. Recirculation zones, which separate from the main flow field, can be further divided into internal recirculation zone and an outer recirculation zone. The temporal interplay of all zones is forming the so-called "vortex breakdown" phenomenon (Wetzel, F., (2007) and Baum, M., Poinsot, T. J., Thevenin, D., (1994) and Staffelbach, G., Poinsot, T., (2006)). Since we are describing counter-rotating movement in relation to

fuel - air, it is important to emphasize the relevance of certain system stability and geometry of the flame. Counter-rotation greatly increases the mixing of fuel with air, and also allows us to change the conventional geometry of the flame. On the other hand, the counter-rotation directly affects the stability of the flame, in conjunction with the relation of the flow velocity and the rate of chemical reactions (Damköhler). Reactions are due to improved homogeneous distribution of the reactive mixture more intense, causing a higher temperature in the core of the flame, and consequently higher thermal NO_x emissions. This can be effectively avoided with the use of a dedicated burner construction, which provides a sufficient internal recirculation of the flue gases in the core of the flame. In comparison with the co-rotation (Figs.7 and 8) the flame of the SF burner is somewhat sensitive to external influences in the combustion chamber (for example, minor pressure changes in the combustion chamber), even if the blow-off of the flame is in fact connected with relatively high swirl number (above 0.8) and the instability of the reactive mixture. For a comparison, Figs.9 and 10are showing the temperature field of co- and counter-rotating system. The flame of co-rotating system is long and narrow, and in principle insensitive to a minor change of swirl number, but due to a poor homogeneous distribution of the reactive mixture unsuitable for use with satisfactory operating parameters (combustion chamber must be properly dimensioned for the complete burnout of the reactants into the products).

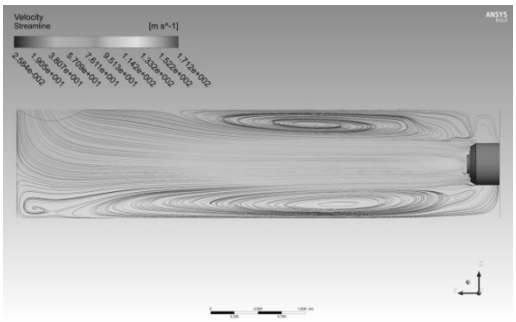

Fig. 7. Co-rotating system.

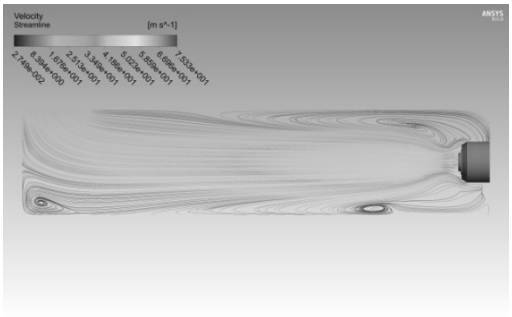

Fig. 8. Counter-rotating system.

Comparison of temperature fields with SF system shows a better symmetry in the co-rotating flame. The question is, of course, to what extent this has a positive impact on the operation of boiler plants (eg. heat transfer). The thermal load on the upper portion (35% of the exchanger surface) of combustion chamber can be significant (up to 60% of the heat energy is released here). In the case of water-tube boilers, the "symmetric" volume load and homogeneous distribution of the reactive mixture is more suitable. This directly coincides with the formation of a flame and its stability under the longitudinal axis of the combustion chamber (Figs. 11-14), depicted in the phase diagrams.

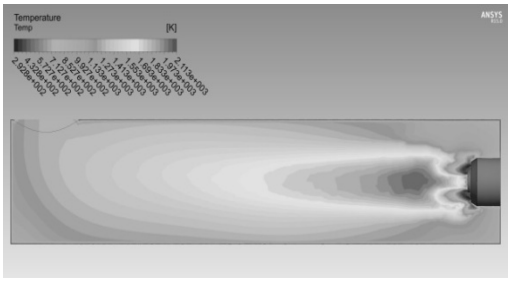

Fig. 9. Co-rotating system – temperature field.

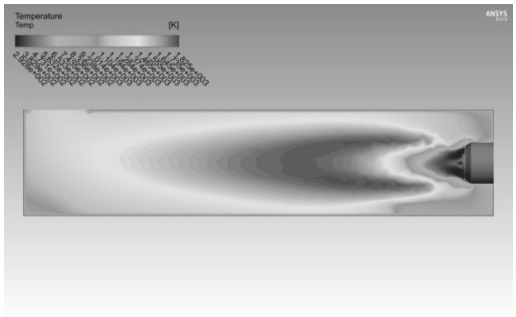

Fig. 10. Counter-rotating system – temperature field.

For easier understanding we can divide the system into internal and external circulation or recirculating area. Internal recirculation field limits and directly dominates the area where the input jet points into the center of the combustion chamber. The example illustrates the comparative analogy between the numerical and experimental data in a longitudinal direction. Internal recirculation area location is slightly different from that obtained by the measurement in the test system. The minima of the functions are in relation with the circular flow of the inner part of the recirculation area, which is entering the combustion chamber with a certain mass flow; they are also an indicator of the strength of the internal recirculation areas.

In the phase diagrams of temperature vs. swirl strength (the swirl strength can be defined similar as the swirl number, but it can also describe the local swirling motion of the vortex), the swirl strength is defined for the counter rotation case (Figs. 11–14) and we can see that the flow conditions in the vicinity of the burner show strong turbulent fluctuations, which are becoming less intensive by moving downstream. However, in the vicinity of the outflow region these fluctuations again become more significant due to oscillatory flow characteristics in the device.

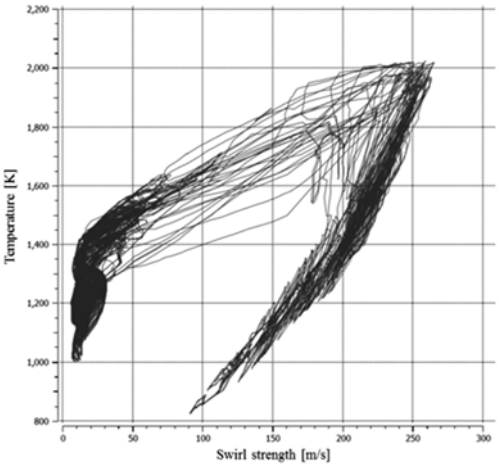

Fig. 11. Diagram temperature-swirl strength (counter rotation point 500mm from burner flange).

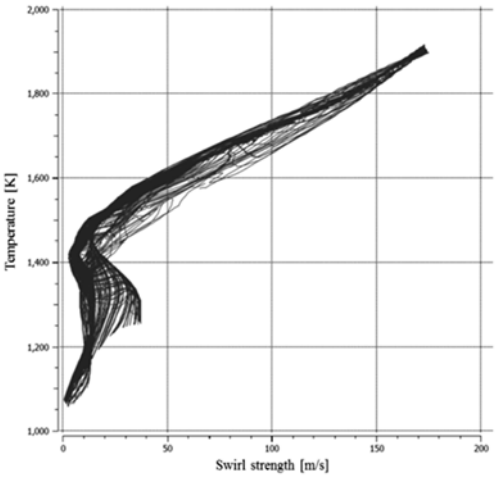

Fig. 12. Diagram temperature-swirl strength (counter rotation point 1500mm from burner flange).

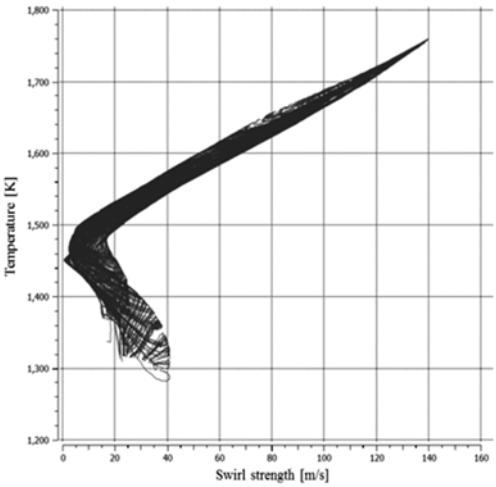

Fig. 13. Diagram temperature-swirl strength (counter rotation point 3000mm from burner flange).

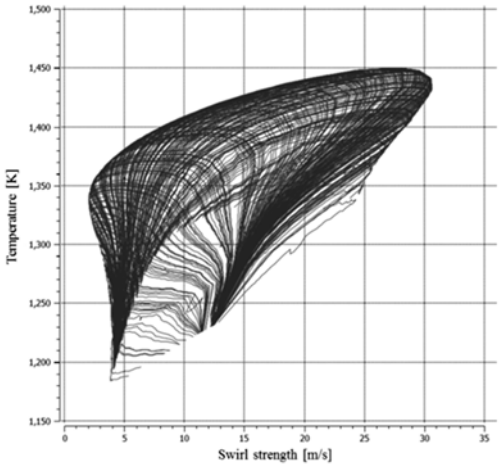

Fig. 14. Diagram temperature-swirl strength (counter rotation point 6000mm from burner flange).

Combustion, regarding to the swirled flow field is based on different factors and mechanisms. An important phenomenon is the heat release from chemical reactions, which leads into local temperature increase and at the same time results in the local decrease of the fluid density, hence again changing the flow field and distribution of the static pressure. For comparison of obtained computational results with experimentally determined case we selected the case with the swirl number S=0,6, which had the best flame characteristics for the observed combustion chamber.

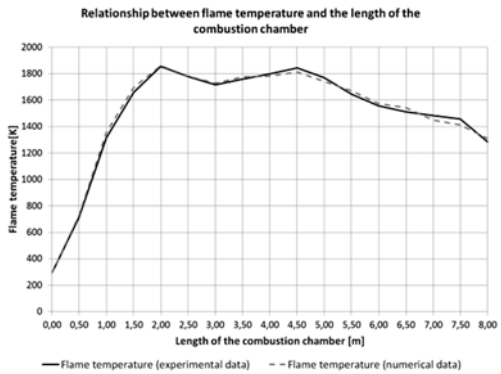

Fig. 15. Relationship between flame temperature (numerical and experimental) and the length of the combustion chamber.

Figure 15presents the relationship of the flame temperature in the axial mid plane of the combustion chamber. The numerical results are showing very good agreement with the experimental data. The computed temperature is following the experimental one with the error range up to max. 6%. The error can be attributed to the limitations in the flow field computation and consequently also to the accuracy of the EDM model, although also a greater care should be taken in assessing the local temperature fluctuations in the locations of the measurements. The error is basically mesh-induced

as the chemistry kinetic requires the detailed discretization of the mesh throughout the computational domain. The intermediate products (as CO) and the products which require activation energy (NO_x), are hence computed with errors as the heat release from the exothermal reactions is not calculated with sufficient resolution. The other part lies in the properties of the EDM model. EDM is known to overestimate the combustion temperature, so the fine tuning (with feedback from experiment) is needed. The same conclusion is valid also for the CO comparison, Fig. 16.

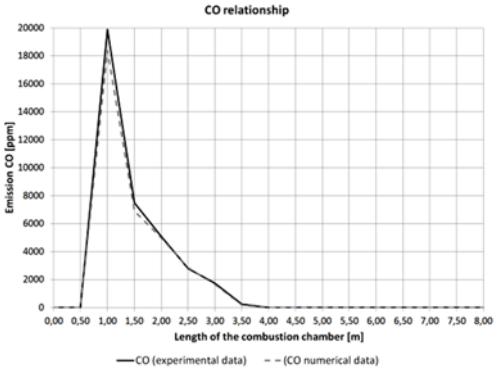

Fig. 16. Relationship between CO emission (numerical and experimental) and the length of the combustion chamber.

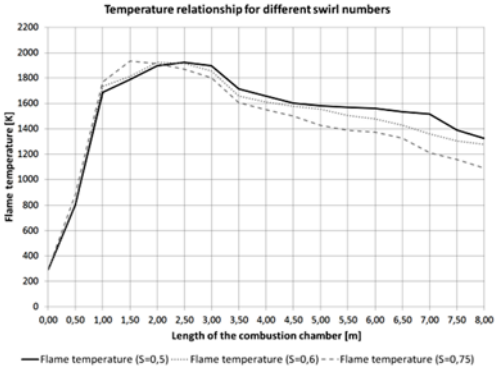

Fig. 17. Temperature along the centerline of the chamber for swirl number values 0.5, 0.6 and 0.75.

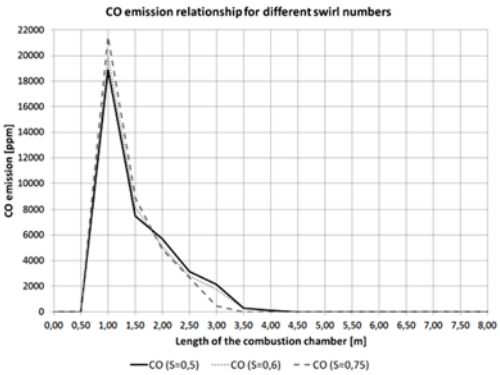

Fig. 18. CO emission along the centerline of the chamber for swirl number values 0.5, 0.6 and 0.75.

In Figs. 17 and 18 comparison of temperature distribution along the centerline of the combustion chamber for three different swirl numbers is shown. A higher swirl number flow shifts the region of high temperatures towards the inlet, resulting in higher CO emissions in the first part of the chamber and lower emissions towards the exit. With lowering the swirl number value, the region of higher temperatures is extended towards the middle of the chamber with the effect of increasing the CO emission in this region in comparison with the case of the high swirl number.

5. CONCLUSION

This work reports on the CFD based combustion simulation of the flow, concentration and the temperature fields in combustion chamber, equipped with a swirling flame burner. The eddy dissipation model in combination with the WALE sub-grid scale LES model leads to very good results in comparison to the experimental results, especially for the mean scalar values (velocity and temperature). The study of increasing the swirl number showed that this leads to the intensification of the recirculation flow in the flame core, reducing temperatures on the outer flame "shell" and hence decreasing thermal NO_x production in the mentioned area. On the other hand, increased the swirl strength is directly responsible for core flame temperature increase; hence increase of thermal NO_x build in the flame core. As shown, swirl flame type burners represent a more efficient way for industrial applications on water tube boilers than a typical burner. For the use in design of improved geometries of the burner the model will be further tested with new generation of SF burners. According to a fact, that there is no practical way of non-field (laboratory) burner testing of 32 MW power and above, the model could find its use as a cost and time efficient way of developing energy efficient and ecological acceptable industrial burner of the future.

REFERENCES

Ansys CFX 14.0 (2011). Solver theory guide.

Aumeier, T. (2011). Die Anwendung eines probabilistischen Partikelmodells fur die Modellierung der turbulenten Verbrennung in Brennkammern, Institut fur Verbrennungstechnik der Luft- und Raumfahrt der Universitat Stuttgart.

Baum, M., T. J. Poinsot and D. Thevenin (1994). Accurate boundary conditions for multispecies reacting flows. *Journal of Computational Physics* 116, 247-261.

Buschulte, W. and W. Wedekamm (1976). Theoretische und experimentelle Untersuchungen von Ölbrennerdüsen; Schadstoffarme Hausheizungen: Systemanalyse; Gentner Verlag Stuttgart. MAN Neue Technologie.

Caraeni, D., C. Bergstrom and L. Fuchs (2000).Modeling of liquid fuel injection, evaporation and mixing in a gas turbine burner using large eddy simulation. *Flow, Turbulence And Combustion*. 65, 223-244.

Faragó, Z. (1985). Kraftstoffaufbereitung und Verbrennung in Brennern. *Symposium Kraftstoffe;Wehrwissenschaftliches Institut für Materialuntersuchungen, Erding.*

Faragó, Z. and A.Baumann (1990). Stabilitätskriterien zur Berechnung der Filmaufbereitung mit Druckdralldüsen; DFVLR.

Faragó, Z. and B.Knapp (2000). Luftunterstützte Druckdralldüse. Projektbericht zum IWO-Projekt Nr. 2000-8 und DLR-Interner- Bericht IB 645 –2000/19.

Gerlinger, P. (2005). *Numerische Verbrennungs simulation*. Springer, Berlin Heidelberg.

Klančišar, M., D. Goebel, T. Schloen, M. Hriberšek and N. Samec (2013).Prediction of mean scalar values and CO-/NOX emissions from confined non-premixed swirl flames with CFD based simulation. *BWK Brennstoff-Wärme-Kraft*10, 38-43.

Klančišar, M., T. Schloen, M. Hriberšek and N. Samec (2015). Analisys and implementation of Large Eddy Simulation in CFD based simulation of confined high swirling flames. *Proceeedings of the European Combustion Meeting.*

Liu, Z. (2010). Square Cylinder Large Eddy Simulation Based on Random Inlet Boundary Condition. *Journal of Applied Fluid Mechanics 3(1), 35-45.*

Möllenbruck, W. (1990). Strömungsprobleme von leichtem Heizöl in Ölfeuerungsanlagen; *DLR IB 643–90/14.*

Parent, J. and Z. Faragó (1986). Theoretical and experimental study on the atomization of fuel oil and simulation fluids with simplex swirl atomizer. *DFVLR IB 643–86/13.*

Poinsot, T. and D. Veynante (2005). *Theoretical and Numerical combustion.* Edwards, Philadelphia.

Ribera, T. and Z. Faragó (1996). Experimental Investigation on Novel Swirl Atomizers, DLR IB 645–96/17. Sprays. *Journal of Applied Fluid Mechanics 3(2), 111-123*

Sridhara, S. N. and B. N. Raghunandan (2010). Photographic Investigations of Jet Disintegration in Airblast

Staffelbach, G. and T. Poinsot (2006).High performance computing for combustion applications. *Super Computing 2006*. Tampa, Florida, USA.

Terao, K., (2007). *Irreversible phenomena–Ignitions, combustion and detonation waves*. Springer-Verlag Berlin Heidelberg.

Vervisch, L. (2005). Turbulent Combustion Modeling, *2005 INRIA Conference Proceedings*, 2-43.

Wetzel, F. (2007). *Numerical investigations for stabilisation of non-premixed, dual swirled flames*. Doctoral dissertation, University of Karlsruhe, Karlsruhe.

Zadravec, M., B. Rajh, N. Samec and M. Hriberšek (2014). Numerical analysis of oil combustion in a small combustion device. *ANALI PAZU 1,41-50.*

Zhang, F., P. Habisreuther, M. Hettel and H. Bockhorn (2009).Modelling of a premixed swirl-stabilized flame using a turbulent flame speed closure model in LES. *Flow Turbulence Combustion* 82,537–5